Available online at www.sciencedirect.com
SCIENCE DIRECT®
International Journal of Thermal Sciences 41 (2002) 1029–1043
International Journal of Thermal Sciences
www.elsevier.com/locate/ijts

Steady-state and transient behaviour of two heat exchangers coupled by a circulating flowstream ☆

Chakkrit Na Ranong *, Wilfried Roetzel

Institut für Thermodynamik, Universität der Bundeswehr Hamburg, D-22039 Hamburg, Germany

Received 2 October 2001; accepted 5 December 2001

Abstract

Systems consisting of two heat exchangers coupled by a circulating flowstream are studied. The systems differ in the flow configurations of the single heat exchangers. For steady-state operation there exists a heat capacity rate of the circulating flowstream which maximizes the temperature changes of the external flowstreams. Until now this optimum has been calculated, assuming that the overall heat transfer coefficients of the heat exchangers do not depend on the mass flow rate of the circulating flowstream. In this paper the dependence of the overall heat transfer coefficient on mass flow rate of the circulating flowstream is taken into account. For transient operating conditions the system response to perturbations of inlet temperatures and mass flow rates is calculated by the method of Laplace-transforms and an explicit finite difference method. The most significant features of the coupled system become apparent considering outlet temperature transients induced by perturbations of the mass flow rate of the circulating flowstream.

Keywords: Coupled heat exchangers; Heat shifting system; Indirect heat transfer; Steady–state optimization; Transient behaviour; Laplace–transformation; Frequency response; Finite difference method; Numerical dissipation; Numerical dispersion

1. Introduction

In almost all power and chemical engineering plants heat exchangers are used as single subunits or as coupled subsystems. Their steady-state behaviour is well known and the calculation methods are highly developed [1,2]. If start-up, shut-down or control processes are considered the knowledge of the transient behaviour becomes important. The transient behaviour of single heat exchangers has already been studied [3,4], but not the transient behaviour of coupled subsystems which are for instance applied to recovering heat in flue gas cleaning plants [5], air conditioning systems [6] and gas turbine plants [7–9].

Subject of this paper is a system which consists of two coupled heat exchangers. The coupling fluid is circulated by a pump. The system is used for transferring heat indirectly from a hot flowstream I to a cold flowstream II. It is called heat shifting system, Fig. 1.

Meierer [5] describes a heat shifting system which is used for heating the pure gases of a flue gas cleaning plant before they enter the chimney. Heat is transferred from the hot raw gases (flowstream I) to the cold pure gases (flowstream II). The circulating fluid is liquid water. The heat shifting system is preferred to a rotating regenerator because pure gases and raw gases are strictly separated and no mixing occurs. Only this solution made it possible to stay within the limit values of contaminant concentration for the pure gases entering the atmosphere.

In air conditioning applications the heat shifting system is used for exchanging heat between outdoor air and exhaust air [6]. In winter the outdoor air is preheated with the exhaust air. In summer the outdoor air is precooled with the exhaust air. The coupled system is advantageous because it does not require exhaust air near outdoor air. The distance is bridged by the circulating flowstream.

☆ The english version of an orally presented German paper on the Internal Meeting of the GVC-Comittee for Heat and Mass Transfer of the VDI (Interne Sitzung des GVC-Fachausschusses Wärme- und Stoffübertragung des VDI) on March 5, 2001, in Bamberg, Germany.

* Corresponding author. Present address: Arbeitsbereich Verfahrenstechnischer Apparatebau, Technische Universität Hamburg Harburg, Eißendorfer Straße 38, D-21073 Hamburg, Germany.

E-mail addresses: c.naranong@tu-harburg.de (Ch. Na Ranong), wilfried.roetzel@unibw-hamburg.de (W. Roetzel).

1290-0729/02/$ – see front matter
PII: S1290-0729(02)01390-X

Nomenclature

A	heat transfer surface	m^2
A_q	cross-sectional area	m^2
a	thermal diffusivity	$m^2 \cdot s^{-1}$
a_{Fou}	Fourier coefficient	
b_{Fou}	Fourier coefficient	
C_0	constant	
c_p	specific isobaric heat capacity	$J \cdot kg^{-1} \cdot K^{-1}$
j	number of Fourier coefficient in Eq. (42)	
k	overall heat transfer coefficient	$W \cdot m^{-2} \cdot K^{-1}$
L_c	characteristic length	m
m	exponent	
Nu	Nußelt number $= \frac{\alpha L_c}{\lambda}$	
NTU	number of transfer units, $\frac{kA}{\dot{W}}$	
n	exponent	
n_{Fou}	number of points for Fourier analysis	
P	dimensionless temperature change of external flowstream	
p	pressure	$N \cdot m^{-2}$
Pr	Prandtl number $= \frac{\nu}{a}$	
$\dot{q}$	heat flux density	$W \cdot m^{-2}$
R	heat capacity rate ratio, e.g., $R_{1\,1,1\,II} = \overline{\dot{W}}_{1\,1}/\overline{\dot{W}}_{1\,II}$	
Re	Reynolds number $= \frac{wL_c}{\nu}$	
s	Laplace parameter	
T	temperature	K
t	time	s
t_B	reference time	s
t_v	initial residence time	s
w	flow velocity	$m \cdot s^{-1}$
$\dot{W}$	heat capacity rate	$W \cdot K^{-1}$
X	length of heat exchanger in the flow direction of external flowstream	m
x	space coordinate	m
Y	length of heat exchanger in the flow direction of circulating flowstream	m
y	space coordinate	m
Z	length of connecting duct	m
z	space coordinate	m

Greek letters

α	heat transfer coefficient	$W \cdot m^{-2} \cdot K^{-1}$
β	expansion coefficient	K^{-1}
ε	dimensionless temperature change of single heat exchanger	
ζ	dimensionless space coordinate $= z/Z$	
η	dimensionless space coordinate $= y/Y$	
θ	dimensionless temperature $= \frac{T - T_{1,\,inII}}{T_{1,\,inI} - T_{1,\,inII}}$	
θ'	dimensionless temperature perturbation $= \frac{T'}{T_{1,\,inI} - T_{1,\,inII}}$	
κ	dimensionless initial residence time	
λ	heat conductivity	$W \cdot m^{-1} \cdot K^{-1}$
ν	kinematic viscosity	$m^2 \cdot s^{-1}$
ξ	dimensionless space coordinate $= x/X$	
ξ_{Gn}	tube friction factor	
ϱ	density	$kg \cdot m^{-3}$
σ	dimensionless flow velocity perturbation	
τ	dimensionless time coordinate $= t/t_B$	
Φ	volumetric dissipation	$W \cdot m^{-3}$
Ω	dimensionless angular frequency	
ω	dimensionless wall parameter	

Super- and subscripts

out	outlet, output
in	inlet, input
k	time-step
l	left connecting duct
M	subscript denoting a subsystem, $M =$ I, II, r, l
opt	optimum
r	right connecting duct
W	wall
1	external flowstream
2	circulating flowstream
I	heat exchanger I
II	heat exchanger II
∞	final steady state

Accents

$'$	perturbation variable
$\bar{}$	initial steady state
$\sim$	Laplace-transform

Other symbols

$\mathcal{I}$	imaginary part of a complex number
$\mathcal{R}$	real part of a complex number

London and Kays [7] consider heat shifting systems in gas turbine plants. Heat is transferred from turbine exhaust gases to compressed combustion air. The circulating fluid is liquid sodium–potassium eutectic alloy. For the first time it is stated that there exists an optimum for the heat capacity rate of the circulating flowstream [7]. Applying this optimum heat capacity rate of the circulating flowstream the largest temperature changes are achieved for given entrance temperatures and heat capacity rates of the external flowstreams. London and Kays [7] consider two coupled counterflow heat exchangers with equal heat capacity rates of the external flowstreams. The overall heat transfer resistances of the heat exchangers are equal and independent of the flow rate of the circulating fluid. In this special case the optimum heat capacity rate of the circulating fluid is equal to the heat capacity rate of the external flowstreams.

Martin [10] and Roetzel [11] consider the optimum for a more general case. The heat capacity rates of the

external flowstreams and the overall heat transfer resistances of the coupled counterflow heat exchangers are arbitrary, but still independent of the flow rate of the circulating flowstream. By means of numerical computations Martin has shown that the optimum heat capacity rate of the circulating flowstream lies between the heat capacity rates of the external flowstreams [10]. Then Roetzel [11] has derived an analytic formula for the calculation of the optimum heat capacity rate. Additionally an economic distribution of the heat transfer area between the two heat exchangers is proposed. Besides counterflow Martin considers cross flow with cross-mixed circulating flowstream. In this case the optimum heat capacity rate is infinitely large [10]. In all the calculations it is assumed that the overall heat transfer coefficient is independent of the circulating flow rate.

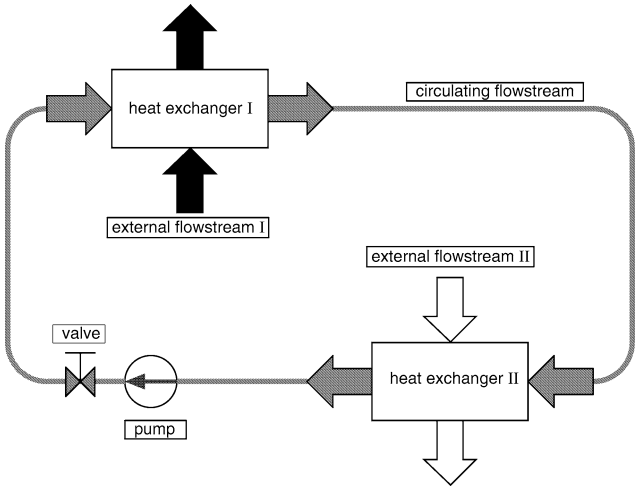

Fig. 1. System of two heat exchangers coupled by a circulating flowstream (cross-flow arrangement). The counterflow arrangement is analogous.

Jansing [12] and Schneider [9] describe a heat shifting system with waste heat boiler installed in a gas turbine plant with combined heat and power generation. Heat is transferred from the hot turbine exhaust gases to the compressed combustion air. Then the turbine exhaust gases enter the waste heat boiler producing heating or process steam. The circulating flow rate determines the distribution of energy between generation of steam and preheating of compressed combustion air. If the circulating flow rate is changed a new operating state will develop. It is of interest after which time the new operating state is reached and how the temperature fields of the system change with time, i.e., the transient behaviour has to be considered. Unlike for the steady state no references are found for the transient behaviour of the coupled system.

In this paper a general calculation method for the steady-state optimization is presented taking into account that the overall heat transfer coefficients depend on the circulating flow rate. This is necessary if the heat transfer resistances on the gas side are decreased by extended surfaces and reach the same order as those on the liquid side, or if the external flowstreams and the circulating flowstream are all liquid. Further it is studied if there exists a finite optimum heat capacity rate of the circulating fluid for other flow configurations than counterflow. Finally calculation methods for the transient behaviour of a heat shifting system are described and examples are discussed.

2. Optimization of steady-state operation

The parameters of the optimization problem are illustrated in Fig. 2. For given inlet temperatures, $T_{1,\,\mathrm{inI}}$ and $T_{1,\,\mathrm{inII}}$, and heat capacity rates of the external flowstreams, $\dot{W}_{1\,\mathrm{I}}$ and $\dot{W}_{1\,\mathrm{II}}$, the heat capacity rate of the circulating

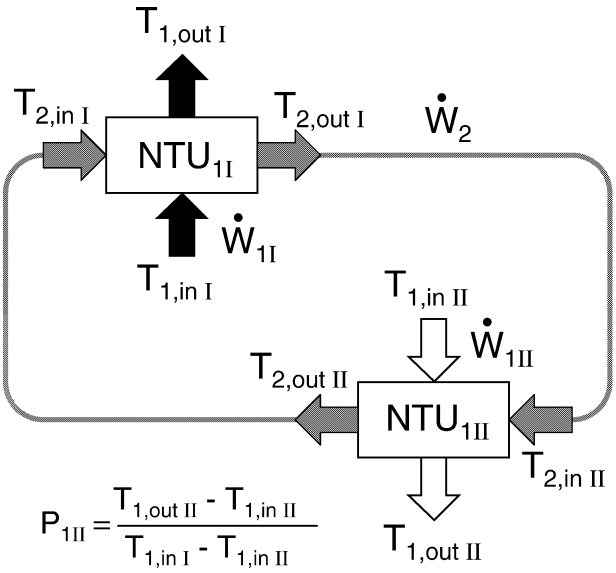

subscripts:

1 : external flowstream
2 : circulating flowstream
I : heat exchanger I
II : heat exchanger II

$$P_{1\mathrm{I}} = \frac{T_{1,\mathrm{in\,I}} - T_{1,\mathrm{out\,I}}}{T_{1,\mathrm{in\,I}} - T_{1,\mathrm{in\,II}}}$$

number of transfer units:

$$NTU_{1\mathrm{I}} = (kA)_{\mathrm{I}} / \dot{W}_{1\mathrm{I}}$$

$$NTU_{1\mathrm{II}} = (kA)_{\mathrm{II}} / \dot{W}_{1\mathrm{II}}$$

Fig. 2. Parameters which are used to describe the system and to determine the optimum circulating flow rate.

fluid $\dot{W}_2$ has to be found which maximizes the temperature changes of the external flowstreams, Fig. 2.

The dimensionless temperature change of flowstream I is given as [7,10]

$$\frac{1}{P_{1\,\mathrm{I}}} = \frac{1}{\varepsilon_{1\,\mathrm{I}}(\mathrm{NTU}_{1\,\mathrm{I}}, R_{2,1\,\mathrm{I}})} + \frac{R_{1\,\mathrm{I},1\,\mathrm{II}}}{\varepsilon_{1\,\mathrm{II}}(\mathrm{NTU}_{1\,\mathrm{II}}, R_{2,1\,\mathrm{II}})} - \frac{1}{R_{2,1\,\mathrm{I}}} \tag{1}$$

i.e.,

$$P_{1\,\mathrm{I}} = P_{1\,\mathrm{I}}(\mathrm{NTU}_{1\,\mathrm{I}}, \mathrm{NTU}_{1\,\mathrm{II}}, R_{2,1\,\mathrm{I}}, R_{1\,\mathrm{I},1\,\mathrm{II}}) \tag{2}$$

because

$$R_{2,1\,\mathrm{II}} = R_{1\,\mathrm{I},1\,\mathrm{II}} R_{2,1\,\mathrm{I}} \tag{3}$$

The heat capacity rate ratio $R_{1\,\mathrm{I},1\,\mathrm{II}}$ is not an independent variable of the optimization problem because the heat capacity rates of both external flowstreams are given.

The temperature changes of the external flowstreams are coupled by the first law

$$R_{1\,\mathrm{I},1\,\mathrm{II}} P_{1\,\mathrm{I}} = P_{1\,\mathrm{II}} \tag{4}$$

If the temperature change of external flowstream I is maximized the temperature change of external flowstream II is also maximized.

The functions

$$\varepsilon_{1\,\mathrm{I}}(\mathrm{NTU}_{1\,\mathrm{I}}, R_{2,1\,\mathrm{I}}) = \frac{T_{1,\,\mathrm{in\,I}} - T_{1,\,\mathrm{out\,I}}}{T_{1,\,\mathrm{in\,I}} - T_{2,\,\mathrm{in\,I}}} \tag{5}$$

and

$$\varepsilon_{1\,\mathrm{II}}(\mathrm{NTU}_{1\,\mathrm{II}}, R_{2,1\,\mathrm{II}}) = \frac{T_{1,\,\mathrm{out\,II}} - T_{1,\,\mathrm{in\,II}}}{T_{2,\,\mathrm{in\,II}} - T_{1,\,\mathrm{in\,II}}} \tag{6}$$

in Eq. (1) are tabulated for a large number of flow configurations in [1]. They characterize the heat exchangers when they are considered as isolated units.

Neglecting wall resistance the overall heat transfer resistance of heat exchanger I is

$$\frac{1}{(kA)_{\mathrm{I}}} = \frac{1}{\alpha_{1\,\mathrm{I}} A_{1\,\mathrm{I}}} + \frac{1}{\alpha_{2\,\mathrm{I}} A_{2\,\mathrm{I}}} \tag{7}$$

Substituting Eq. (7) into the definition of $\mathrm{NTU}_{1\,\mathrm{I}}$ given in Fig. 2 yields

$$\frac{1}{\mathrm{NTU}_{1\,\mathrm{I}}} = \frac{\dot{W}_{1\,\mathrm{I}}}{\alpha_{1\,\mathrm{I}} A_{1\,\mathrm{I}}} + \frac{\dot{W}_2}{\alpha_{2\,\mathrm{I}} A_{2\,\mathrm{I}}} \frac{1}{R_{2,1\,\mathrm{I}}} \tag{8}$$

The two dimensionless groups in Eq. (8) are abbreviated by

$$N_{1\,\mathrm{I}} = \frac{\alpha_{1\,\mathrm{I}} A_{1\,\mathrm{I}}}{\dot{W}_{1\,\mathrm{I}}} \quad \text{and} \quad N_{2\,\mathrm{I}} = \frac{\alpha_{2\,\mathrm{I}} A_{2\,\mathrm{I}}}{\dot{W}_2} \tag{9}$$

yielding

$$\frac{1}{\mathrm{NTU}_{1\,\mathrm{I}}} = \frac{1}{N_{1\,\mathrm{I}}} + \frac{1}{N_{2\,\mathrm{I}} R_{2,1\,\mathrm{I}}} \tag{10}$$

Assuming constant fluid properties the varying heat transfer coefficients do not influence each other. Taking into account that all data of the external flowstreams, the flow configurations and the constant fluid properties of the circulating flowstream are given, $\mathrm{NTU}_{1\,\mathrm{I}}$ is reduced to a function of $Re_{2\,\mathrm{I}}$ alone, substituting

$$N_{2\,\mathrm{I}} = Nu(Re_{2\,\mathrm{I}}, Pr_2) \frac{A_{2\,\mathrm{I}}}{A_{q2\,\mathrm{I}}} Re_{2\,\mathrm{I}}^{-1} Pr_2^{-1} \tag{11}$$

$$R_{2,1\,\mathrm{I}} = \frac{\lambda_2}{\lambda_{1\,\mathrm{I}}} \frac{L_{c1\,\mathrm{I}}}{L_{c2\,\mathrm{I}}} \frac{A_{q2\,\mathrm{I}}}{A_{q1\,\mathrm{I}}} \frac{Re_{2\,\mathrm{I}}}{Re_{1\,\mathrm{I}}} \frac{Pr_2}{Pr_{1\,\mathrm{I}}} \tag{12}$$

into Eq. (10). In the same way $\mathrm{NTU}_{1\,\mathrm{II}}$ is reduced to a function of $Re_{2\,\mathrm{II}}$. The Reynolds numbers are coupled by the continuity equation

$$Re_{2\,\mathrm{II}} = \frac{A_{q2\,\mathrm{I}}}{A_{q2\,\mathrm{II}}} \frac{L_{c2\,\mathrm{II}}}{L_{c2\,\mathrm{I}}} Re_{2\,\mathrm{I}} \tag{13}$$

Thus the dimensionless temperature change of external flowstream I, $P_{1\,\mathrm{I}}$, is a function of $Re_{2\,\mathrm{I}}$ which is the only independent variable

$$P_{1\,\mathrm{I}} = P_{1\,\mathrm{I}}(Re_{2\,\mathrm{I}}) \tag{14}$$

The problem is reduced to finding the optimum Reynolds number $Re_{2\,\mathrm{I}}^{\mathrm{opt}}$ of the circulating flowstream of heat exchanger I analytically, graphically or numerically. If the function $P_{1\,\mathrm{I}}(Re_{2\,\mathrm{I}})$ is differentiable the necessary and sufficient conditions for relative maxima are

$$\frac{\mathrm{d}P_{1\,\mathrm{I}}}{\mathrm{d}Re_{2\,\mathrm{I}}} = 0 \tag{15}$$

and

$$\frac{\mathrm{d}^2 P_{1\,\mathrm{I}}}{\mathrm{d}Re_{2\,\mathrm{I}}^2} < 0, \tag{16}$$

respectively. At the transition points from laminar to turbulent flow the function $P_{1\,\mathrm{I}}(Re_{2\,\mathrm{I}})$ is not differentiable. Comparing the numerical values of $P_{1\,\mathrm{I}}$ at the relative maxima and at the transition points the absolute maximum is finally obtained.

2.1. Examples

Applying the presented method the optimum circulating flow rate is calculated for a system consisting of two identical finned tube heat exchangers, operated with equal heat capacity rates of the external flowstreams. The heat exchangers are described by Kays and London [8] as pure cross-flow units. The circulating fluid is water. Heat is indirectly transferred from a hot external airstream I to a cold external airstream II. Eqs. (12)–(12) for heat exchanger I and the corresponding equations for heat exchanger II are

$$\begin{aligned} N_{1\,\mathrm{I}} &= N_{1\,\mathrm{II}} = N_1 = 2.965 \\ N_{2\,\mathrm{I}} &= N_{2\,\mathrm{II}} = N_2 = 244.0 \frac{Nu_2(Re_2, Pr_2 = 7.01)}{Re_2} \\ R_{2,1\,\mathrm{I}} &= R_{2,1\,\mathrm{II}} = R_{2,1} = 1.735 \times 10^{-3} Re_2 \end{aligned} \tag{17}$$

In the turbulent region the Nußselt number of the circulating water Nu_2 is calculated using the Gnielinski equation [1]

$$Nu_2 = \frac{\frac{\xi_{Gn}}{8}(Re_2 - 1000)\,Pr_2}{1 + 12.7\sqrt{\frac{\xi_{Gn}}{8}}(Pr^{2/3} - 1)} \tag{18}$$

$$\xi_{Gn} = (1.82\log_{10}Re_2 - 1.64)^{-2}, \quad 2300 \leqslant Re_2 \leqslant 10^6 \tag{19}$$

In the laminar region it is necessary to take into account the thermal boundary conditions at the heat transfer surface [13]. To simplify the calculation it is assumed that the Nußselt number for fully developed laminar flow with constant surface heat flux density can be used. The numerical value is

$$Nu_2 = 4.36 \tag{20}$$

For the considered system consisting of two identical heat exchangers operated with equal external heat capacity rates Eqs. (1) and (2) reduce to

$$\frac{1}{P_1} = \frac{2}{\varepsilon_1(\mathrm{NTU}_1, R_{2,1})} - \frac{1}{R_{2,1}} \tag{21}$$

and

$$P_1 = P_1(\mathrm{NTU}_1, R_{2,1}), \tag{22}$$

respectively. Eq. (22) can be visualized as a surface in three dimensions. However, to obtain numerical values a two-dimensional contour plot is more suitable. Such a plot is given in Fig. 3. Lines with constant dimensionless temperature change of the external flowstreams P_1 are plotted as contour lines. If the overall heat transfer coefficients are independent of the heat capacity rate ratio $R_{2,1}$ the intersection between the horizontal line $\mathrm{NTU}_1 = \text{const}$ and the contour line with the largest possible numerical value of P_1 gives the optimum. This is exemplified for $\mathrm{NTU}_1 = 12$ in Fig. 3.

For the considered finned tube heat exchangers the NTUs are not constant, but strongly depend on the heat capacity rate ratio $R_{2,1}$. The optimum lies on a curve which represents the correct relationship between NTU_1 and $R_{2,1}$, Fig. 3. This curve is called operation characteristic. NTU_1 significantly changes from 1.14 to 2.58 as the heat capacity rate ratio is increased from 0 to 10. The largest numerical value of P_1 lies at the upper bound of the interval $0 \leqslant R_{2,1} \leqslant 10$. The single finned tube heat exchangers are designed for a heat capacity rate ratio $R_{2,1} = 8.2$. This is also reasonable for the coupled system. The operation point lies in the turbulent region with high temperature changes of the external flowstreams. Perturbations of the circulating flow rate hardly change the outlet temperatures of the external flowstreams, Fig. 3.

The situation is different for heat exchangers with large heat transfer areas and therefore large NTUs. This is clarified by virtually enlarging the heat transfer areas of the considered finned tube heat exchangers by the factor 5. The new operation characteristic is plotted in Fig. 3. There exists an absolute maximum of P_1 at a heat capacity rate ratio $R_{2,1} = 1.13$. The optimum heat capacity rate of the circulating fluid is slightly larger than the heat capacity rate of the external flowstreams.

Because the contour plots are quite descriptive they are also discussed for three other flow configurations, Figs. 4, 5 and 6. It is assumed that the operation characteristic

$$\mathrm{NTU}_1 = \mathrm{NTU}_1(R_{2,1}) \tag{23}$$

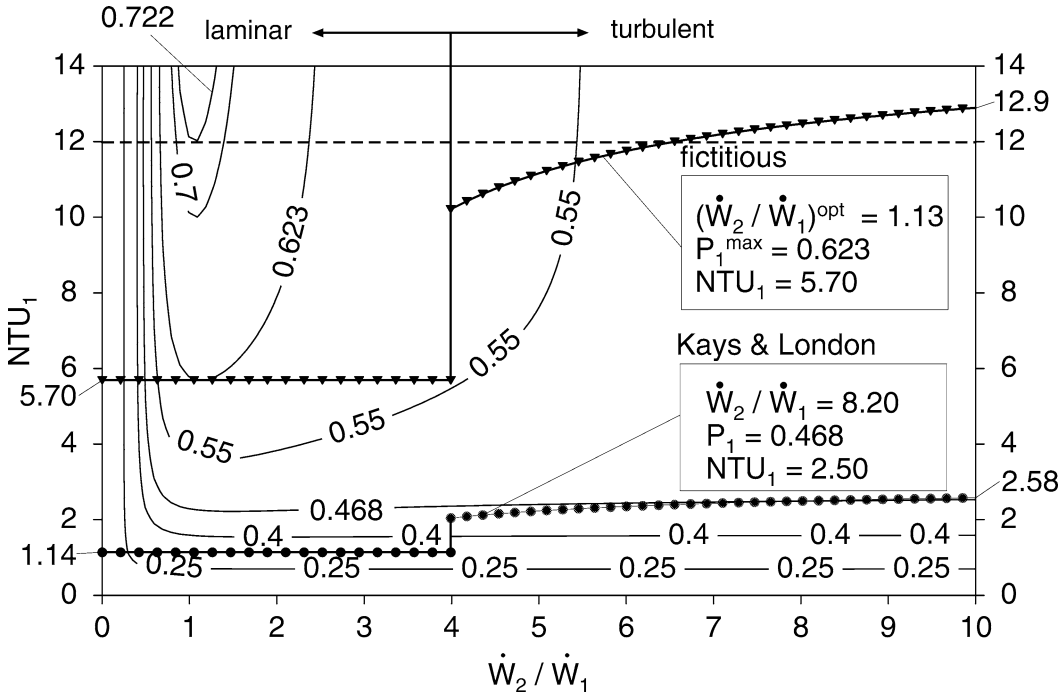

Fig. 3. Contour plot for two coupled cross-flow heat exchangers with pure cross flow. Labeled solid lines are contour lines with $P_1 = \text{const}$. The dashed line represents the case $\mathrm{NTU}_1 = 12$. The operation characteristic of two coupled finned tube heat exchangers after Kays and London is marked with circles. Additionally an operation characteristic for large resulting NTUs is marked with triangles.

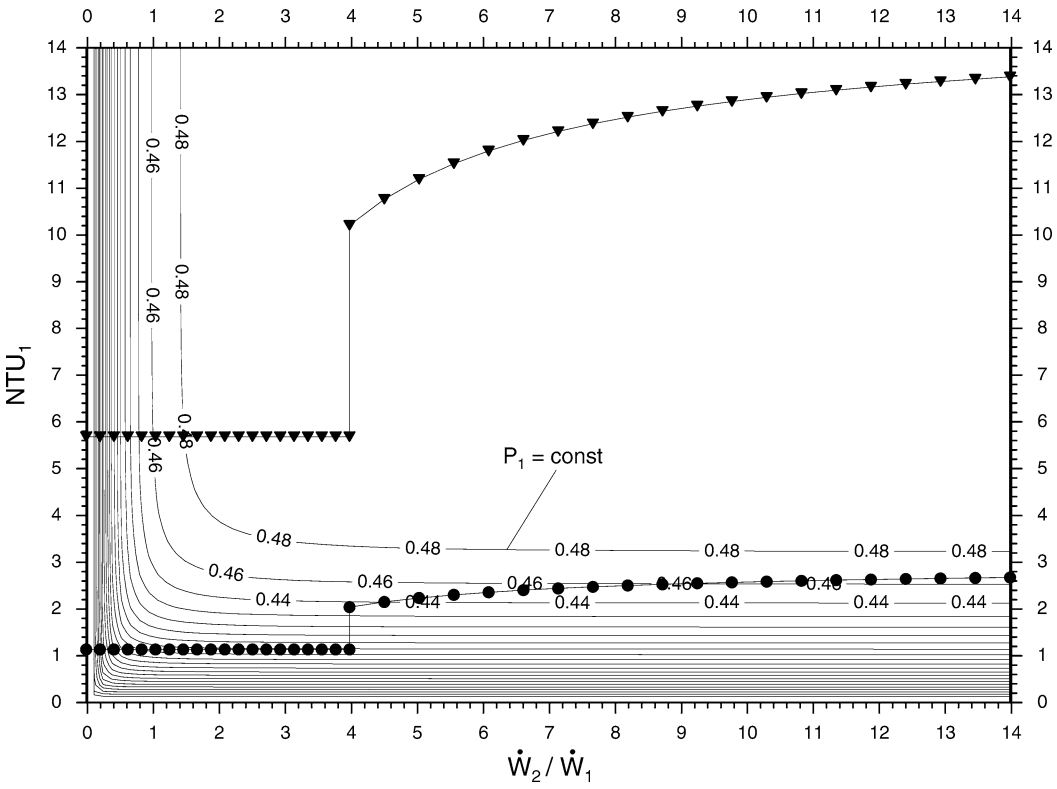

Fig. 4. Contour plot for two coupled cross-flow heat exchangers with cross-mixed circulating flowstream. Labeled solid lines are contour lines with $P_1 = \text{const}$. The operation characteristic with small resulting NTUs is marked with circles. The operation characteristic with large resulting NTUs marked with triangles.

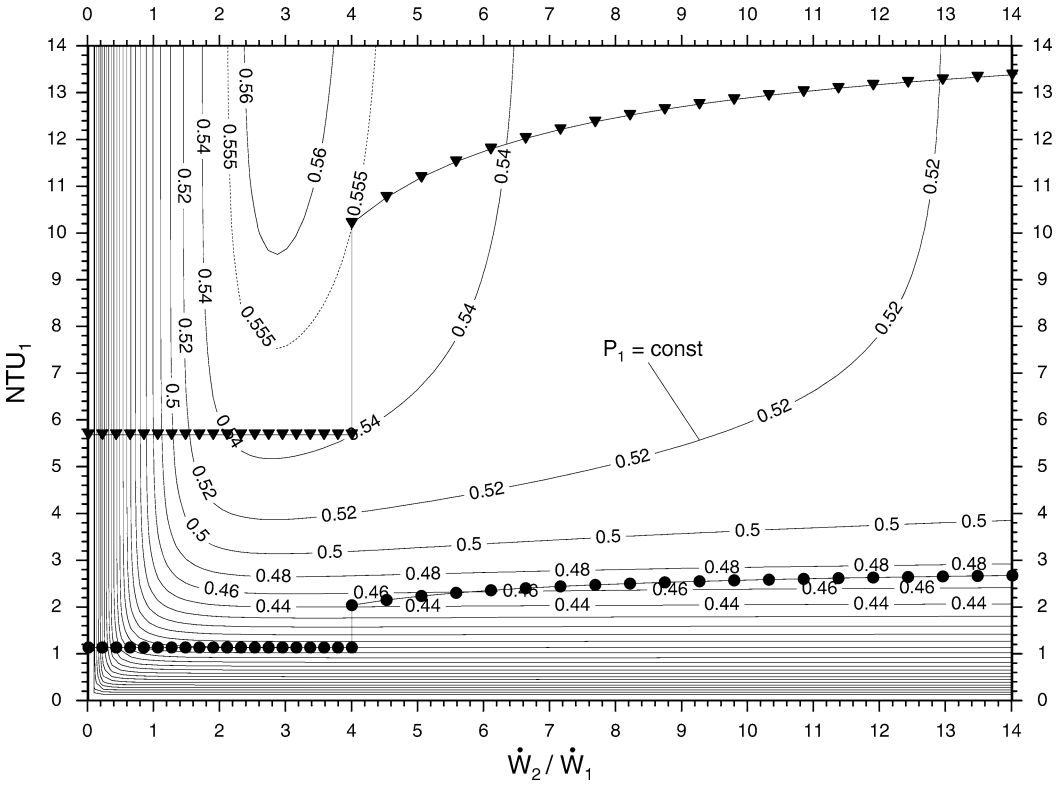

Fig. 5. Contour plot for two coupled cross-flow heat exchangers with cross-mixed external flowstreams. Labeled solid lines are contour lines with $P_1 = \text{const}$. The operation characteristic with small resulting NTUs is marked with circles. The operation characteristic with large resulting NTUs is marked with triangles.

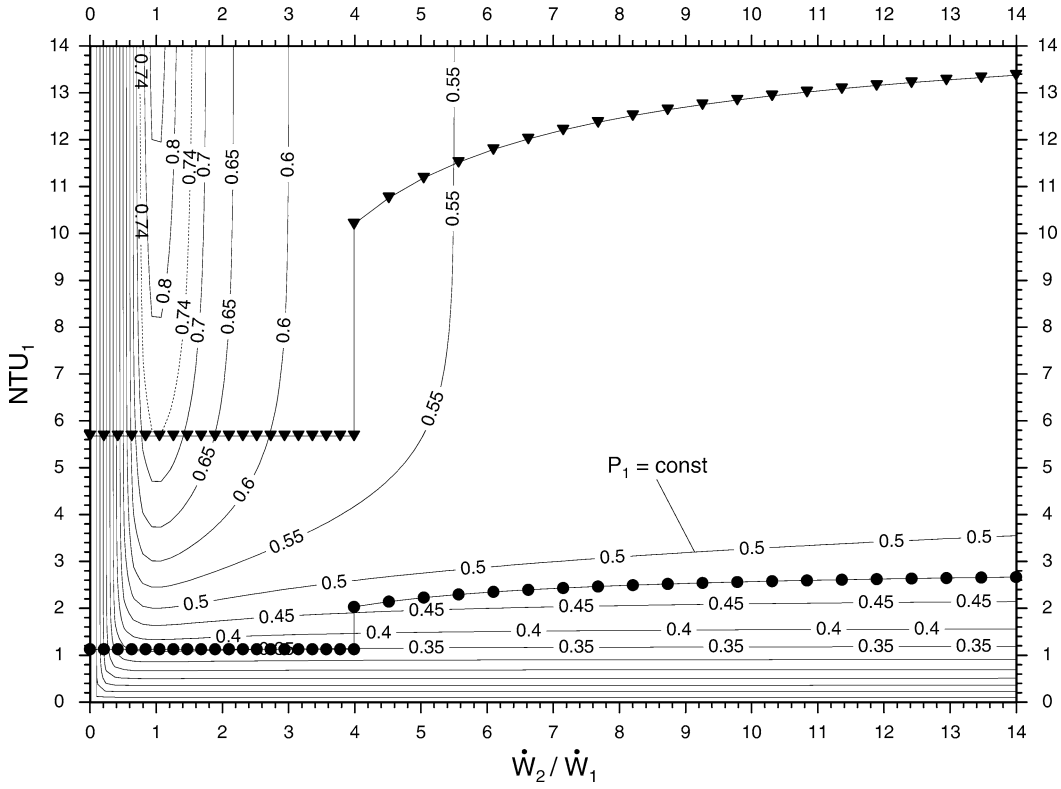

Fig. 6. Contour plot for two coupled counterflow heat exchangers. Labeled solid lines are contour lines with $P_1 = \text{const}$. The operation characteristic with small resulting NTUs is marked with circles. The operation characteristic with large resulting NTUs is marked with triangles.

which is plotted in Fig. 3 is also realizable for the other flow configurations.

For cross flow with cross-mixed circulating flowstream, Fig. 4, the contour lines are monotonically decaying. The optimum circulating flow rate is always infinite because the operation characteristics are horizontal or rising curves. For cross flow with cross-mixed external flowstreams and small resulting NTUs the largest value of P_1 lies at the upper bound of the considered interval $0 \leqslant R_{2,1} \leqslant 14$, Fig. 5. For large resulting NTUs the optimum lies at the laminar-turbulent transition point with $R_{2,1}^{\text{opt}} = 3.99$ and $P_1^{\max} = 0.555$, Fig. 5. For counterflow and small resulting NTUs there is a weak optimum with $R_{2,1}^{\text{opt}} = 10.2$ and $P_1^{\max} = 0.477$ and for large resulting NTUs a strong one with $R_{2,1}^{\text{opt}} = 1$ and $P_1^{\max} = 0.740$, Fig. 6.

3. Transient behaviour

The transient behaviour is studied for three systems with different flow configurations of the coupled heat exchangers, Fig. 7. Each system has five input signals and two output signals. The five input signals are:

(1) perturbation of the inlet temperature of external flowstream I;
(2) perturbation of the inlet temperature of external flowstream II;
(3) mass flow rate perturbation of external flowstream I;
(4) mass flow rate perturbation of external flowstream II;
(5) mass flow rate perturbation of the circulating flowstream.

The two output signals are:

(1) outlet temperature of external flowstream I;
(2) outlet temperature of external flowstream II.

For control applications disturbances occurring during steady-state operation are of great importance. Therefore a steady-state operating condition is chosen as the initial state. To calculate the transients of the output signals a suitable mathematical description of the processes is necessary. This description is based on the energy equation for general flow processes [4]

$$\varrho c_p \frac{\mathrm{D}T}{\mathrm{D}t} = -\nabla \cdot \vec{q} + \beta T \frac{\mathrm{D}p}{\mathrm{D}t} + \Phi \tag{24}$$

The energy equation is simplified by introducing adiabatic mixing temperatures and heat transfer coefficients. The following assumptions are made:

- All fluids are incompressible.
- Specific heat capacities and thermophysical fluid properties are constant.
- Plug flow is present in both heat exchangers and in the connecting ducts.

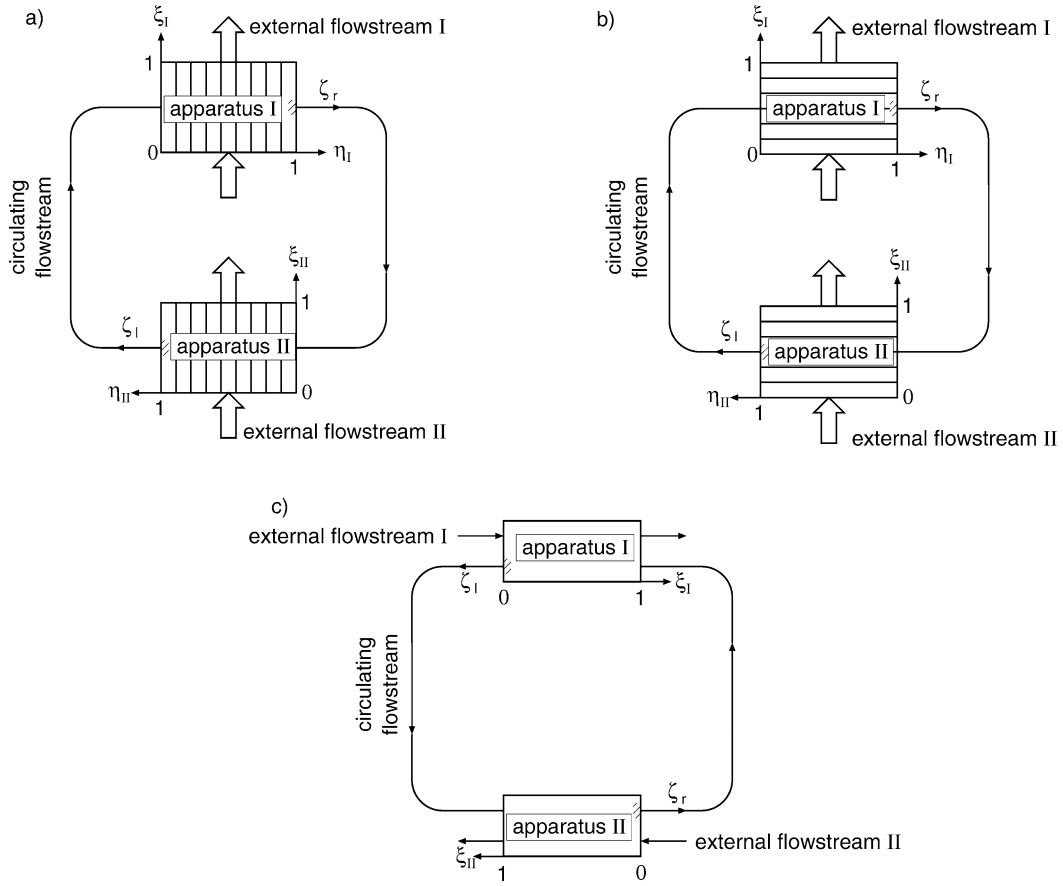

Fig. 7. Coordinate systems and flow configurations of the considered systems: (a) cross flow with cross-mixed circulating flowstream, (b) cross flow with cross-mixed external flowstreams, (c) counterflow.

- Local heat transfer coefficients are spatially constant, but may change with time due to mass flow rate perturbations.
- Thermal conductivity of solid walls perpendicular to the flow direction is infinite.
- There is no heat conduction or mixing in the flow direction.
- Dissipation of mechanical power and heat losses to the surroundings are negligible.

Application of the energy Eq. (24) yields a hyperbolic system of partial differential equations (PDEs). With the corresponding initial, boundary and coupling conditions these PDEs describe the temperature fields of the system and especially the outlet temperatures which are the output signals of interest. For transient studies of processes with an initial steady-state operating condition it is useful to look at changes of variables away from their initial steady-state value instead of the absolute variables. These changes are called perturbation variables. Their initial values are all equal to zero, yielding homogeneous initial conditions. The perturbation technique is applied to temperatures, flow velocities and heat transfer coefficients.

$$T(t) = \overline{T} + T'(t) \tag{25}$$

$$w(t) = \overline{w} + w'(t) \tag{26}$$

$$\alpha(t) = \overline{\alpha} + \alpha'(t) \tag{27}$$

Using the empirical correlation for the Nußselt number

$$Nu = C_0 Re^m Pr^n \tag{28}$$

the perturbation of the heat transfer coefficient becomes a function of the flow velocity perturbation

$$\alpha' = \left[\left(1 + \frac{w'}{\overline{w}}\right)^m - 1\right]\overline{\alpha} \tag{29}$$

The resulting governing equations are given in Appendix A in dimensionless form. If the perturbation variables are small the energy equations can be linearized [14] around the initial steady state, Appendix A. The boundary and coupling conditions are given in Appendix B.

3.1. Solution methods

The coupled systems of PDEs are solved by the method of Laplace-transforms and an explicit finite difference method. If the coefficients of the PDEs are constant both methods are applied. If the coefficients depend on time, only the finite difference method is applicable.

The coefficients of the linearized energy equations are always constant. In general the coefficients of the exact

energy equations depend on time. They are only constant if all mass flow rates are constant or if there is a simultaneous step change of all mass flow rates at the begin of the process.

3.1.1. Method of Laplace-transforms

The Laplace-transform of a function $f(\tau)$ in the interval $0 \leqslant \tau \leqslant \infty$ is defined as [15]

$$\mathcal{L}\{f(\tau)\} = \tilde{f}(s) = \int_0^\infty \mathrm{e}^{-s\tau} f(\tau)\,\mathrm{d}\tau \tag{30}$$

The energy equations with constant coefficients, the boundary and the coupling conditions are transformed with respect to the dimensionless time coordinate from the time domain into the frequency domain. The transformation rules are summarized by Spiegel [16]. In the frequency domain solution methods for ordinary differential equations (ODEs) become applicable. The numerical inversion algorithm of Honig [17] is used for obtaining the final solution in the time domain.

3.1.2. Finite difference method

The partial differential equations are approximated with finite difference equations. The terms of the energy equations are expressed combining values of the variables and parameters at discrete points of a computational grid. To keep the method explicit and the truncation errors small, a combination of the FTBS-scheme (forward time and backward space) [18] and Wendroff's scheme is chosen [19].

An important special case occurs if the external flowstreams are gaseous and the circulating flowstream is liquid. Normally the residence time of the gas is much smaller than the residence time of the liquid [8]

$$t_{v1} \ll t_{v2} \tag{31}$$

If the initial residence time of the liquid is chosen as reference time

$$t_B = t_{v2} \tag{32}$$

the time derivatives in the energy equations for the external flowstreams, Appendix A, vanish because

$$\kappa_1 = \frac{t_{v1}}{t_B} \approx 0 \tag{33}$$

The gas temperatures develop without inertia effects, i.e., their history is insignificant. Therefore it is not reasonable to approximate the space derivative with Wendroff's scheme which requires values at two different points of time. Instead the three-point-formula is used [18].

Besides the problem of numerical stability, numerical dispersion and numerical dissipation can make the calculation results useless without being recognized. To derive criteria for the generation of computational grids where the effects of numerical dispersion and dissipation are minimized the simplified PDE with constant coefficients

$$-(1+\sigma)\frac{\partial\theta'}{\partial\xi} = \kappa\frac{\partial\theta'}{\partial\tau} \tag{34}$$

is considered. Eq. (34) reflects the transport properties of the energy equations in the flow direction. The dimensionless flow velocity perturbation σ in Eq. (34) is a constant, i.e., the criterion is derived for a time step with $\sigma^k = \sigma$. The superscript k denotes the discrete time coordinate. If σ changes a new criterion holds and a new computational grid has to be generated. Solutions of Eq. (34) show neither dispersion nor dissipation [18]. A dispersion and dissipation analysis of the FTBS-scheme and Wendroff's scheme approximating Eq. (34) shows that dispersion and dissipation diminish for

$$\frac{\Delta\xi}{\Delta\tau} = \frac{\kappa}{1+\sigma} \tag{35}$$

or with dimensions

$$\frac{\Delta x}{\Delta t} = \overline{w} + w'(t) \tag{36}$$

Eq. (35) is applied to discretize the space and time coordinates. For a given time discretization Δt the discretization of the space coordinate depends on the velocity of the fluid flowing in the direction of this space coordinate, Eq. (36). For counterflow there are two criteria for the discretization of a single space coordinate, Fig. 7, if the flow velocities of external and circulating flowstream are different. Therefore the calculation is simultaneously conducted on two computational grids for each time step.

To apply the method of Laplace-transforms and the finite difference method the inhomogeneous parts of the energy equations, Appendix A, which contain the temperature fields of the initial steady state have to be known before the transient calculation starts. The equations for the steady-state temperature fields, the solution in the frequency domain and the finite difference schemes will be published separately due to their extent [20].

3.2. Examples

The most significant properties of the coupled system reveal if the mass flow rate of the circulating flowstream is perturbed. For comparison the same parameters in the governing equations, Appendix A, have been chosen for the three systems in Fig. 7:

$$\overline{N}_{1\mathrm{I}} = \overline{N}_{1\mathrm{II}} = 8, \qquad m_{1\mathrm{I}} = m_{1\mathrm{II}} = 0.8$$
$$\overline{N}_{2\mathrm{I}} = \overline{N}_{2\mathrm{II}} = 12, \qquad m_{2\mathrm{I}} = m_{2\mathrm{II}} = 0.8$$
$$R_{2,1\mathrm{I}} = R_{2,1\mathrm{II}} = 4, \qquad \kappa_{1\mathrm{I}} = \kappa_{1\mathrm{II}} = 0$$
$$\kappa_{2\mathrm{I}} = \kappa_{2\mathrm{II}} = 1, \qquad \omega_{\mathrm{I}} = \omega_{\mathrm{II}} = 5$$
$$\overline{N}_{2\mathrm{r}} = \overline{N}_{2\mathrm{l}} = 1, \qquad m_{2\mathrm{r}} = m_{2\mathrm{l}} = 0.8$$
$$\kappa_{2\mathrm{r}} = \kappa_{2\mathrm{l}} = 10, \qquad \omega_{\mathrm{r}} = \omega_{\mathrm{l}} = 1$$

Fig. 8 shows the system response to a mass flow rate perturbation of the circulating fluid. Due to the continuity equation the dimensionless flow velocity perturbations of the

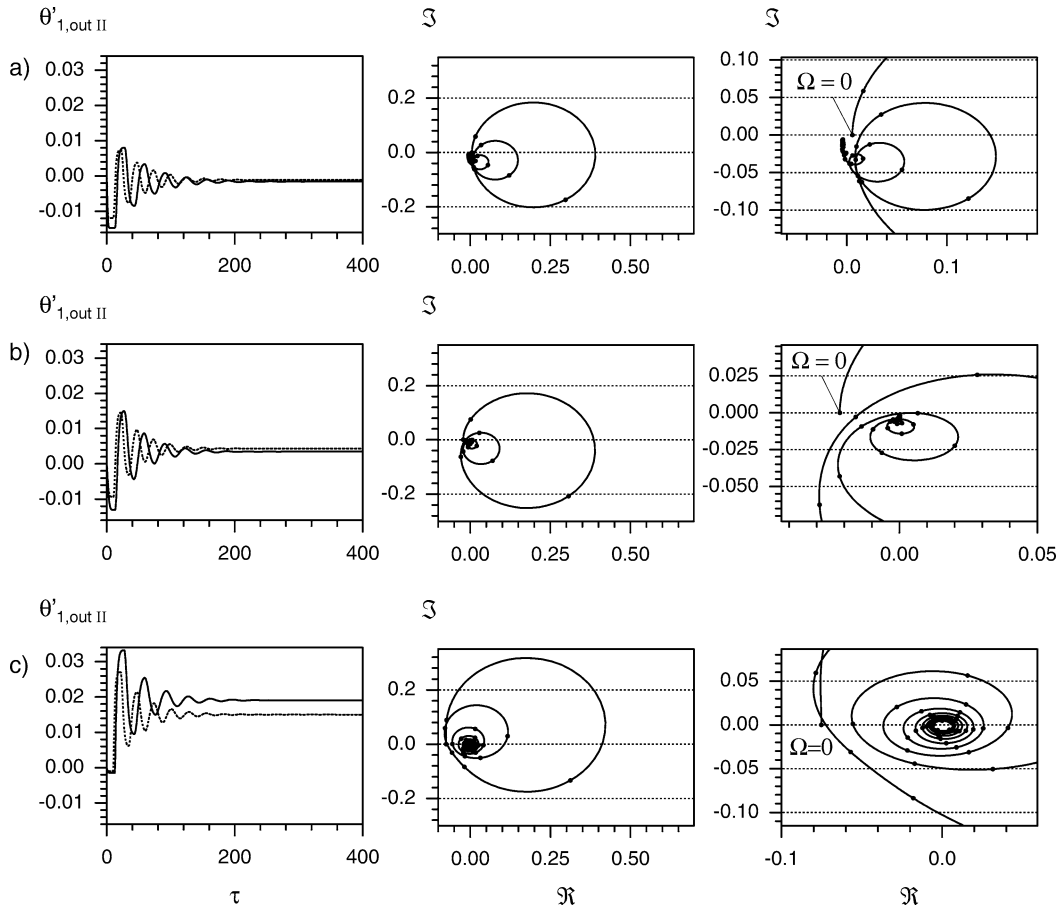

Fig. 8. System response to a perturbation of the mass flow rate of the circulating flowstream. (a) cross flow with cross-mixed circulating flowstream, (b) cross flow with cross-mixed external flowstreams, (c) counterflow. Left: Step response. Solid lines denote solution of exact energy equations. Dashed lines denote solution of linearized energy equations. Center and right: Frequency responses. The interval between two marked dimensionless angular frequencies is $\Delta\Omega = 2\pi/50$.

circulating flowstream are equal for both heat exchangers and both connecting ducts:

$$\frac{w'_{2\,\mathrm{I}}}{\overline{w}_{2\,\mathrm{I}}} = \frac{w'_{2\,\mathrm{II}}}{\overline{w}_{2\,\mathrm{II}}} = \frac{w'_{2\mathrm{r}}}{\overline{w}_{2\mathrm{r}}} = \frac{w'_{2\mathrm{l}}}{\overline{w}_{2\mathrm{l}}} = \sigma_2 \tag{37}$$

On the left of Fig. 8 the step response to the input signal $\sigma_2 = -0.2$ is shown. The output signal $\theta'_{1,\mathrm{outII}}$ oscillates with decaying amplitude until a new steady state is reached. A temperature oscillation, induced by a step change of mass flow rate, does not exist for the subsystems when they are considered separately. The period of the damped oscillation is influenced by the circulation time of the coupling fluid after the step change and the heat capacities of the system.

Another important property of coupled heat exchangers becomes apparent if the final steady-state values of the output signal $\theta'_{1,\mathrm{outII}}$ are considered, Table 1. The sign of the final steady-state value is positive for counterflow and cross flow with cross-mixed external flowstreams, while it is negative for cross flow with cross-mixed circulating flowstream. Decreasing the mass flow rate of the circulating liquid can both increase and decrease the outlet temperature of external flowstream II, depending on the flow configuration of the heat exchangers and the operating condition at the initial steady state.

Table 1
Comparison of the final steady-state values for the exact and linearized energy equations. The inlet signal is a drop of the mass flow rate of the circulating liquid with $\sigma_2 = -0.2$

	$\theta'^{\mathrm{exact}}_{1,\,\mathrm{outII}}(\tau \to \infty)$	$\theta'^{\mathrm{lin}}_{1,\,\mathrm{outII}}(\tau \to \infty)$
Cross flow with cross-mixed circulating flowstream	−0.00154227	−0.00110672
Cross flow with cross-mixed external flowstreams	+0.00346866	+0.00432710
Counterflow	+0.0190972	+0.0150339

The solutions of the exact and linearized energy equations are shifted in time, left of Fig. 8. Perturbations of the circulating system propagate in the flow direction with flow velocity of the circulating fluid. This is correctly modeled by the exact energy equations, but not by the linearized ones. Analyzing the characteristics of the exact and linearized en-

Table 2
Dimensionless propagation velocities of information in the flow direction of the circulating flowstream for the exact and linearized energy equations

Subsystem	Definition of propagation velocity	Linearized energy equations	Exact energy equations
Cross flow	$\frac{d\eta}{d\tau}$	$\frac{1}{\kappa_2}$	$\frac{1+\sigma_2(\tau)}{\kappa_2}$
Counterflow	$\frac{d\xi}{d\tau}$	$-\frac{1}{\kappa_2}$	$-\frac{1+\sigma_2(\tau)}{\kappa_2}$
Duct flow	$\frac{d\zeta}{d\tau}$	$\frac{1}{\kappa_2}$	$\frac{1+\sigma_2(\tau)}{\kappa_2}$

ergy equations which are both of the hyperbolic type yields the dimensionless propagation velocities of information, Table 2. To recognize if these dimensionless propagation velocities are physically correct they are reformulated with dimensions. For cross flow the propagation velocity of information of the linearized energy equations is wrong.

$$\frac{d\eta}{d\tau} = \frac{1}{\kappa_2} \Longrightarrow \frac{t_B}{Y}\frac{dy}{dt} = \frac{1}{t_{v2}/t_B} \Longrightarrow \frac{dy}{dt} = \bar{w}_2 \tag{38}$$

Perturbations always propagate with the flow velocity of the initial steady state, although the flow velocity is varying with time. The propagation velocity of information of the exact energy equations is correct because it is identical to the flow velocity.

$$\frac{d\eta}{d\tau} = \frac{1+\sigma_2}{\kappa_2} \Longrightarrow \frac{t_B}{Y}\frac{dy}{dt} = \frac{1+w_2'(t)/\bar{w}_2}{t_{v2}/t_B}$$
$$\Longrightarrow \frac{dy}{dt}(t) = \bar{w}_2 + w_2'(t) \tag{39}$$

After the drop of the circulating mass flow rate the correct propagation velocities of the exact energy equations are smaller than the incorrect ones of the linearized energy equations. This explains the phase shift in Fig. 8. The maxima and minima of the solution of the linearized energy equations occur to early because they propagate to fast.

If the inlet signal is a harmonic oscillation the system response is a harmonic oscillation with the same frequency as the inlet signal—after initial transients—provided the linearized energy equations are applied to describing the process. Amplitude and phase of the system response are given by the frequency response [21]. The frequency response is the sector $s = \mathcal{I}\Omega$ of the transfer function

$$\widetilde{G}_{1\,\mathrm{II},\sigma 2} = \frac{\tilde{\theta}'_{1,\,\mathrm{outII}}(s)}{\tilde{\sigma}_2(s)} \tag{40}$$

and depicted in the complex plane as a curve parametrized by the dimensionless angular frequency Ω. The curve starts with $\Omega = 0$ and ends with $\Omega \to \infty$ in the origin of the complex plane. The distance between the origin and a point on the curve, multiplied by the amplitude of the input signal, gives the amplitude of the output signal. The angle between the abscissa and the connecting line between origin and a point on the curve gives the phase of the output signal.

To verify calculation results the limit theorems of Laplace-transformation are applied. Graphically they can be interpreted as a relation between frequency response and unit step response [22]. The initial value theorem says that the final value of the unit step response at $\tau \to \infty$ is equal to the amplitude of the frequency response at $\Omega = 0$. Therefore on the right of Fig. 8 the region around $\Omega = 0$ is zoomed. The final value theorem says that the initial value of the unit step response is equal to the amplitude of the frequency response at $\Omega \to \infty$.

Table 3
Numerical values of the Fourier coefficients $a_{\mathrm{Fou},0}$

	$\frac{1}{2}a_{\mathrm{Fou},0}$
Cross flow with cross-mixed circulating flowstream	−0.0124377
Cross flow with cross-mixed external flowstreams	−0.0110430
Counterflow	−0.0140313

If the mass flow rate perturbations are arbitrary the finite difference method has to be applied to solve the exact energy equations. The system response to a pulsating circulating flowstream is considered. The input signal is

$$\sigma_2 = 0.6\sin\left(\frac{2\pi}{22}\tau\right) \tag{41}$$

After initial transients the output signal of the system is periodic, Fig. 9. For comparison the solution of the linearized energy equations is plotted with dashed lines. Despite the large amplitude of the perturbation both solutions are in good agreement. The right part of Fig. 9 shows the Fourier analysis of the solution of the exact energy equations. The exact output signal is approximated with the finite Fourier series

$$\theta'_{1,\,\mathrm{outII}}(\tau) \approx \frac{1}{2}a_{\mathrm{Fou},0} + \sum_{j=1}^{n_{\mathrm{Fou}}-1}\left[a_{\mathrm{Fou},j}\frac{\cos 2\pi j\frac{\tau}{\Delta\tau_{\mathrm{Fou}}}}{n_{\mathrm{Fou}}} + b_{\mathrm{Fou},j}\frac{\sin 2\pi j\frac{\tau}{\Delta\tau_{\mathrm{Fou}}}}{n_{\mathrm{Fou}}}\right] + \frac{1}{2}a_{\mathrm{Fou},\frac{n}{2}}\cos\pi\frac{\tau}{\Delta\tau_{\mathrm{Fou}}} \tag{42}$$

where $n_{\mathrm{Fou}} = 4096$ and $\Delta\tau_{\mathrm{Fou}} = 396/12288$. While the solution of the linearized energy equations is a harmonic oscillation with the same frequency as the inlet signal around the mean zero, the solution of the exact energy equations oscillates with the fundamental frequency $\Omega = 2\pi/22$, but with integer multiples of the fundamental frequency superimposed, Fig. 9.

Crucial is that the solution oscillates around a mean which is different from zero, Table 3,

$$a_{\mathrm{Fou},0} \neq 0 \tag{43}$$

A pulsating circulating flowstream changes the time averaged behaviour of the system. This fact is not represented by the linearized energy equations.

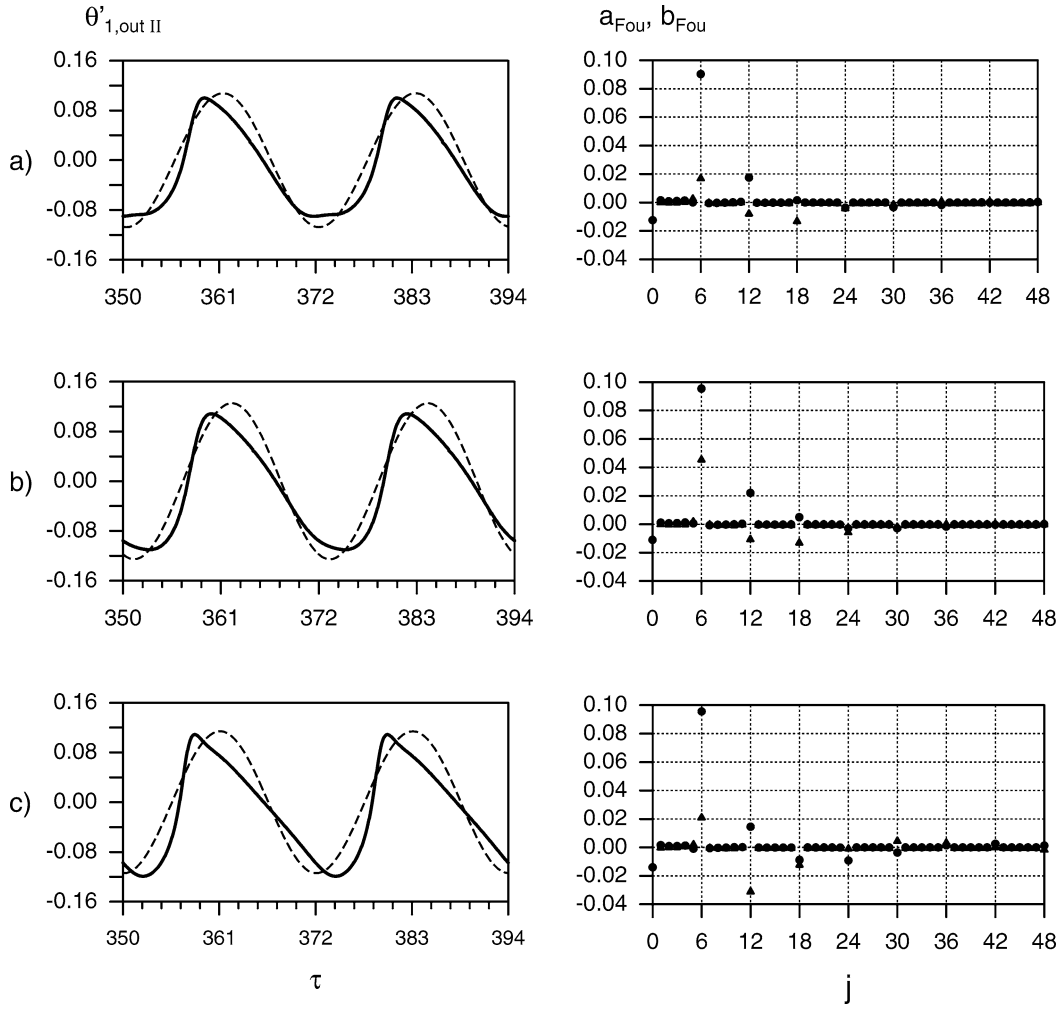

Fig. 9. System response to a harmonic perturbation of the mass flow rate of the circulating liquid, Eq. (42). (a) cross flow with cross-mixed circulating flowstream, (b) cross flow with cross-mixed external flowstreams, (c) counterflow. Left: Outlet temperature perturbations of external flowstream II. Solid lines denote solution of exact energy equations. Dashed lines denote solution of linearized energy equations. Right: Fourier analysis. The Fourier coefficients a_{Fou} are marked with circles and b_{Fou} with triangles.

4. Conclusions

If constant NTUs are assumed for the calculation of the optimum circulating heat capacity rate one has to be careful because NTUs are only constant in special cases, i.e., if the heat transfer resistance of the circulating flowstream is negligible or if the heat transfer coefficients of the circulating flowstream are independent of flow velocity. Here a general method is presented which takes into account that NTUs may depend on the heat capacity rate of the circulating flowstream. A finite optimum circulating flow rate exists for counterflow, cross flow with cross-mixed circulating flowstream and pure cross flow as flow configurations of the single heat exchangers. For cross flow with cross-mixed circulating flowstream the optimum heat capacity rate is always infinite.

Due to its internal circulation the coupled system shows a different transient behaviour than single heat exchangers. This becomes most apparent considering system responses to step changes of the mass flow rate of the circulating fluid. The outlet temperatures oscillate with decaying amplitude until a new steady state is reached. A temperature oscillation, induced by a step change of mass flow rate, does not exist for the considered single heat exchangers.

Appendix A. Governing equations

The dimensionless parameters of the governing equations are defined as follows:

$$\overline{N}_{1M} = \frac{\bar{\alpha}_{1M} A_{1M}}{\overline{\dot{W}}_{1M}} \qquad N'_{1M}(\tau) = \frac{\alpha'_{1M} A_{1M}}{\overline{\dot{W}}_{1M}}$$

$$R_{2,1M} = \frac{\overline{\dot{W}}_2}{\overline{\dot{W}}_{1M}}$$

$$\sigma_{1M}(\tau) = \frac{w'_{1M}}{\bar{w}_{1M}}, \qquad \kappa_{1M} = \frac{t_{v,1M}}{t_B} \quad \text{mit } M = \mathrm{I}, \mathrm{II}$$

$$\overline{N}_{2M} = \frac{\bar{\alpha}_{2M} A_{2M}}{\overline{\dot{W}}_{2M}}, \qquad N'_{2M}(\tau) = \frac{\alpha'_{2M} A_{2M}}{\overline{\dot{W}}_{2M}}$$

$$\sigma_2(\tau) = \frac{w'_{2M}}{\bar{w}_{2M}}, \qquad \kappa_{2M} = \frac{t_{v,2M}}{t_B} \quad \text{mit } M = \mathrm{I, II, r, l}$$

$$\omega_{\mathrm{I}} = \frac{C_{W\mathrm{I}}}{C_{1\mathrm{I}}}\kappa_{1\mathrm{I}}, \qquad \omega_{\mathrm{II}} = \frac{C_{W\mathrm{II}}}{C_{1\,\mathrm{II}}}\kappa_{1\,\mathrm{II}}$$

$$\omega_{\mathrm{r}} = \frac{C_{W\mathrm{r}}}{C_{2\mathrm{r}}}\kappa_{2\mathrm{r}}, \qquad \omega_{\mathrm{l}} = \frac{C_{W\mathrm{l}}}{C_{2\mathrm{l}}}\kappa_{2\mathrm{l}}$$

With these parameters, Eq. (29) results in

$$N'_{1M} = \left[(1+\sigma_{1M})^{m_{1M}} - 1\right]\overline{N}_{1M} \quad M = \mathrm{I, II} \tag{A.1}$$

$$N'_{2M} = \left[(1+\sigma_2)^{m_{2M}} - 1\right]\overline{N}_{2M} \quad M = \mathrm{I, II, r, l} \tag{A.2}$$

Eqs. (A.1) and (A.2) reflects that perturbations of heat transfer coefficients depend on flow velocity perturbations.

A.1 Cross flow with cross-mixed circulating flowstream

A.1.1 Exact energy equations

External flowstream:

$$-(1+\sigma_{1M})\frac{\partial\theta'_{1M}}{\partial\xi_M} - \left(\overline{N}_{1M} + N'_{1M}\right)\left(\theta'_{1M} - \theta'_{\mathrm{W}M}\right) - \left(N'_{1M} - \sigma_{1M}\overline{N}_{1M}\right)\left(\bar{\theta}_{1M} - \bar{\theta}_{\mathrm{W}M}\right) = \kappa_{1M}\frac{\partial\theta'_{1M}}{\partial\tau} \tag{A.3}$$

Circulating flowstream:

$$-(1+\sigma_2)\frac{\partial\theta'_{2M}}{\partial\eta_M} - \left(\overline{N}_{2M} + N'_{2M}\right)\left(\theta'_{2M} - \int_0^1 \theta'_{\mathrm{W}M}\,\mathrm{d}\xi_M\right) - \left(N'_{2M} - \sigma_2\overline{N}_{2M}\right)\left(\bar{\theta}_{2M} - \int_0^1 \bar{\theta}_{\mathrm{W}M}\,\mathrm{d}\xi_M\right) = \kappa_{2M}\frac{\partial\theta'_{2M}}{\partial\tau} \tag{A.4}$$

Wall equation:

$$N'_{1M}\left(\bar{\theta}_{1M} - \bar{\theta}_{\mathrm{W}M}\right) + \left(\overline{N}_{1M} + N'_{1M}\right)\left(\theta'_{1M} - \theta'_{\mathrm{W}M}\right) + N'_{2M}R_{2,1M}\left(\bar{\theta}_{2M} - \bar{\theta}_{\mathrm{W}M}\right) + \left(\overline{N}_{2M} + N'_{2M}\right)R_{2,1M}\left(\theta'_{2M} - \theta'_{\mathrm{W}M}\right) = \omega_M\frac{\partial\theta'_{\mathrm{W}M}}{\partial\tau} \tag{A.5}$$

A.1.2 Linearized energy equations

External flowstream:

$$-\frac{\partial\theta'_{1M}}{\partial\xi_M} - \overline{N}_{1M}\left(\theta'_{1M} - \theta'_{\mathrm{W}M}\right) - (m_{1M}-1)\overline{N}_{1M}\left(\bar{\theta}_{1M} - \bar{\theta}_{\mathrm{W}M}\right)\sigma_{1M} = \kappa_{1M}\frac{\partial\theta'_{1M}}{\partial\tau} \tag{A.6}$$

Circulating flowstream:

$$-\frac{\partial\theta'_{2M}}{\partial\eta_M} - \overline{N}_{2M}\left(\theta'_{2M} - \int_0^1 \theta'_{\mathrm{W}M}\,\mathrm{d}\xi_M\right) - (m_{2M}-1)\overline{N}_{2M}\left(\bar{\theta}_{2M} - \int_0^1 \bar{\theta}_{\mathrm{W}M}\,\mathrm{d}\xi_M\right)\sigma_2 = \kappa_{2M}\frac{\partial\theta'_{2M}}{\partial\tau} \tag{A.7}$$

Wall equation:

$$m_{1M}\overline{N}_{1M}\left(\bar{\theta}_{1M} - \bar{\theta}_{\mathrm{W}M}\right)\sigma_{1M} + \overline{N}_{1M}\left(\theta'_{1M} - \theta'_{\mathrm{W}M}\right) + m_{2M}\overline{N}_{2M}R_{2,1M}\left(\bar{\theta}_{2M} - \bar{\theta}_{\mathrm{W}M}\right)\sigma_2 + \overline{N}_{2M}R_{2,1M}\left(\theta'_{2M} - \theta'_{\mathrm{W}M}\right) = \omega_M\frac{\partial\theta'_{\mathrm{W}M}}{\partial\tau} \tag{A.8}$$

A.2 Cross flow with cross-mixed external flowstreams

A.2.1 Exact energy equations

External flowstream:

$$-(1+\sigma_{1M})\frac{\partial\theta'_{1M}}{\partial\xi_M} - \left(\overline{N}_{1M} + N'_{1M}\right)\left(\theta'_{1M} - \int_0^1 \theta'_{\mathrm{W}M}\,\mathrm{d}\eta_M\right) - \left(N'_{1M} - \sigma_{1M}\overline{N}_{1M}\right)\left(\bar{\theta}_{1M} - \int_0^1 \bar{\theta}_{\mathrm{W}M}\,\mathrm{d}\eta_M\right) = \kappa_{1M}\frac{\partial\theta'_{1M}}{\partial\tau} \tag{A.9}$$

Circulating flowstream:

$$-(1+\sigma_2)\frac{\partial\theta'_{2M}}{\partial\eta_M} - \left(\overline{N}_{2M} + N'_{2M}\right)\left(\theta'_{2M} - \theta'_{\mathrm{W}M}\right) - \left(N'_{2M} - \sigma_{2M}\overline{N}_{2M}\right)\left(\bar{\theta}_{2M} - \bar{\theta}_{\mathrm{W}M}\right) = \kappa_{2M}\frac{\partial\theta'_{2M}}{\partial\tau} \tag{A.10}$$

Wall equation:

$$N'_{1M}\left(\bar{\theta}_{1M} - \bar{\theta}_{\mathrm{W}M}\right) + \left(\overline{N}_{1M} + N'_{1M}\right)\left(\theta'_{1M} - \theta'_{\mathrm{W}M}\right) + N'_{2M}R_{2,1}\left(\bar{\theta}_{2M} - \bar{\theta}_{\mathrm{W}M}\right) + \left(\overline{N}_{2M} + N'_{2M}\right)R_{2,1}\left(\theta'_{2M} - \theta'_{\mathrm{W}M}\right) = \omega_M\frac{\partial\theta'_{\mathrm{W}M}}{\partial\tau} \tag{A.11}$$

A.2.2 Linearized energy equations

External flowstream:

$$-\frac{\partial\theta'_{1M}}{\partial\xi_M} - \overline{N}_{1M}\left(\theta'_{1M} - \int_0^1 \theta'_{\mathrm{W}M}\,\mathrm{d}\eta_M\right) - (m_{1M}-1)\overline{N}_{1M}\left(\bar{\theta}_{1M} - \int_0^1 \bar{\theta}_{\mathrm{W}M}\,\mathrm{d}\eta_M\right)\sigma_{1M} = \kappa_{1M}\frac{\partial\theta'_{1M}}{\partial\tau} \tag{A.12}$$

Circulating flowstream:

$$-\frac{\partial\theta'_{2M}}{\partial\eta_M} - \overline{N}_{2M}\left(\theta'_{2M} - \theta'_{\mathrm{W}M}\right) - (m_{2M}-1)\overline{N}_{2M}\left(\bar{\theta}_{2M} - \bar{\theta}_{\mathrm{W}M}\right)\sigma_2 = \kappa_{2M}\frac{\partial\theta'_{2M}}{\partial\tau} \tag{A.13}$$

Wall equation:

$$m_{1M}\overline{N}_{1M}(\bar{\theta}_{1M}-\bar{\theta}_{WM})\sigma_{1M}+\overline{N}_{1M}(\theta'_{1M}-\theta'_{WM})+m_{2M}\overline{N}_{2M}R_{2,1}(\bar{\theta}_{2M}-\bar{\theta}_{WM})\sigma_2+\overline{N}_{2M}R_{2,1}(\theta'_{2M}-\theta'_{WM})=\omega_M\frac{\partial\theta'_{WM}}{\partial\tau} \quad (A.14)$$

A.3 Counterflow

A.3.1 Exact energy equations

External flowstream:

$$-(1+\sigma_{1M})\frac{\partial\theta'_{1M}}{\partial\xi_M}-(\overline{N}_{1M}+N'_{1M})(\theta'_{1M}-\theta'_{WM})-(N'_{1M}-\sigma_{1M}\overline{N}_{1M})(\bar{\theta}_{1M}-\bar{\theta}_{WM})=\kappa_{1M}\frac{\partial\theta'_{1M}}{\partial\tau} \quad (A.15)$$

Circulating flowstream:

$$(1+\sigma_2)\frac{\partial\theta'_{2M}}{\partial\xi_M}-(\overline{N}_{2M}+N'_{2M})(\theta'_{2M}-\theta'_{WM})-(N'_{2M}-\sigma_{2M}\overline{N}_{2M})(\bar{\theta}_{2M}-\bar{\theta}_{WM})=\kappa_{2M}\frac{\partial\theta'_{2M}}{\partial\tau} \quad (A.16)$$

Wall equation:

$$N'_{1M}(\bar{\theta}_{1M}-\bar{\theta}_{WM})+(\overline{N}_{1M}+N'_{1M})(\theta'_{1M}-\theta'_{WM})+N'_{2M}R_{2,1M}(\bar{\theta}_{2M}-\bar{\theta}_{WM})+(\overline{N}_{2M}+N'_{2M})R_{2,1M}(\theta'_{2M}-\theta'_{WM})=\omega_M\frac{\partial\theta'_{WM}}{\partial\tau} \quad (A.17)$$

A.3.2 Linearized energy equations

External flowstream:

$$-\frac{\partial\theta'_{1M}}{\partial\xi_M}-\overline{N}_{1M}(\theta'_{1M}-\theta'_{WM})-(m_{1M}-1)\overline{N}_{1M}(\bar{\theta}_{1M}-\bar{\theta}_{WM})\sigma_{1M}=\kappa_{1M}\frac{\partial\theta'_{1M}}{\partial\tau} \quad (A.18)$$

Circulating flowstream:

$$\frac{\partial\theta'_{2M}}{\partial\xi_M}-\overline{N}_{2M}(\theta'_{2M}-\theta'_{WM})-(m_{2M}-1)\overline{N}_{2M}(\bar{\theta}_{2M}-\bar{\theta}_{WM})\sigma_2=\kappa_{2M}\frac{\partial\theta'_{2M}}{\partial\tau} \quad (A.19)$$

Wall equation:

$$m_{1M}\overline{N}_{1M}(\bar{\theta}_{1M}-\bar{\theta}_{WM})\sigma_{1M}+\overline{N}_{1M}(\theta'_{1M}-\theta'_{WM})+m_{2M}\overline{N}_{2M}R_{2,1M}(\bar{\theta}_{2M}-\bar{\theta}_{WM})\sigma_2+\overline{N}_{2M}R_{2,1M}(\theta'_{2M}-\theta'_{WM})=\omega_M\frac{\partial\theta'_{WM}}{\partial\tau} \quad (A.20)$$

A.4 Connecting ducts

A.4.1 Exact energy equations

Circulating flowstream:

$$-(1+\sigma_2)\frac{\partial\theta'_{2M}}{\partial\zeta_M}-(\overline{N}_{2M}+N'_{2M})(\theta'_{2M}-\theta'_{WM})=\kappa_{2M}\frac{\partial\theta'_{2M}}{\partial\tau} \quad (A.21)$$

Wall equation:

$$(\overline{N}_{2M}+N'_{2M})(\theta'_{2M}-\theta'_{WM})=\omega_M\frac{\partial\theta'_{WM}}{\partial\tau} \quad (A.22)$$

A.4.2 Linearized energy equations

Circulating flowstream:

$$-\frac{\partial\theta'_{2M}}{\partial\zeta_M}-\overline{N}_{2M}(\theta'_{2M}-\theta'_{WM})=\kappa_{2M}\frac{\partial\theta'_{2M}}{\partial\tau} \quad (A.23)$$

Wall equation:

$$\overline{N}_{2M}(\theta'_{2M}-\theta'_{WM})=\omega_M\frac{\partial\theta'_{WM}}{\partial\tau} \quad (A.24)$$

Appendix B. Boundary and coupling conditions

The boundary and coupling conditions are formulated using the coordinate systems introduced in Fig. 7.

B.1 Cross flow with cross-mixed circulating flowstream

Boundary conditions:

$$\theta'_{1\,I}(\xi_I=0,\eta_I,\tau)=\theta'_{1,\,inI}(\tau) \quad (B.1)$$

$$\theta'_{1\,II}(\xi_{II}=0,\eta_{II},\tau)=\theta'_{1,\,inII}(\tau) \quad (B.2)$$

Coupling conditions:

$$\theta'_{2\,I}(\eta_I=1,\tau)=\theta'_{2r}(\zeta_r=0,\tau) \quad (B.3)$$

$$\theta'_{2r}(\zeta_r=1,\tau)=\theta'_{2\,II}(\eta_{II}=0,\tau) \quad (B.4)$$

$$\theta'_{2\,II}(\eta_{II}=1,\tau)=\theta'_{2l}(\zeta_l=0,\tau) \quad (B.5)$$

$$\theta'_{2l}(\zeta_l=1,\tau)=\theta'_{2\,I}(\eta_I=0,\tau) \quad (B.6)$$

B.2 Cross flow with cross-mixed external flowstreams

Boundary conditions:

$$\theta'_{1\,I}(\xi_I=0,\tau)=\theta'_{1,\,inI}(\tau) \quad (B.7)$$

$$\theta'_{1\,II}(\xi_{II}=0,\tau)=\theta'_{1,\,inII}(\tau) \quad (B.8)$$

Coupling conditions:

$$\int_0^1\theta'_{2\,I}(\xi_I,\eta_I=1,\tau)\,d\xi_I=\theta'_{2r}(\zeta_r=0,\tau) \quad (B.9)$$

$$\theta'_{2r}(\zeta_r=1,\tau)=\theta'_{2\,II}(\xi_{II},\eta_{II}=0,\tau) \quad (B.10)$$

$$\int_0^1 \theta'_{2\,\mathrm{II}}(\xi_{\mathrm{II}}, \eta_{\mathrm{II}} = 1, \tau)\,\mathrm{d}\xi_{\mathrm{II}} = \theta'_{2\mathrm{l}}(\zeta_{\mathrm{l}} = 0, \tau) \tag{B.11}$$

$$\theta'_{2\mathrm{l}}(\zeta_{\mathrm{l}} = 1, \tau) = \theta'_{2\,\mathrm{I}}(\xi_{\mathrm{I}}, \eta_{\mathrm{I}} = 0, \tau) \tag{B.12}$$

B.3 Counterflow

Boundary conditions:

$$\theta'_{1\,\mathrm{I}}(\xi_{\mathrm{I}} = 0, \tau) = \theta'_{1,\,\mathrm{inI}}(\tau) \tag{B.13}$$

$$\theta'_{1\,\mathrm{II}}(\xi_{\mathrm{II}} = 0, \tau) = \theta'_{1,\,\mathrm{inII}}(\tau) \tag{B.14}$$

Coupling conditions:

$$\theta'_{2\,\mathrm{I}}(\xi_{\mathrm{I}} = 0, \tau) = \theta'_{2\mathrm{l}}(\zeta_{\mathrm{l}} = 0, \tau) \tag{B.15}$$

$$\theta'_{2\mathrm{r}}(\zeta_{\mathrm{l}} = 1, \tau) = \theta'_{2\,\mathrm{II}}(\xi_{\mathrm{II}} = 1, \tau) \tag{B.16}$$

$$\theta'_{2\,\mathrm{II}}(\xi_{\mathrm{II}} = 0, \tau) = \theta'_{2\mathrm{r}}(\zeta_{\mathrm{r}} = 0, \tau) \tag{B.17}$$

$$\theta'_{2\mathrm{l}}(\zeta_{\mathrm{r}} = 1, \tau) = \theta'_{2\,\mathrm{I}}(\xi_{\mathrm{I}} = 1, \tau) \tag{B.18}$$

References

[1] VDI Wärmeatlas, Berechnungsblätter für den Wärmeübergang, 7th edn., VDI Verlag, Düsseldorf, 1994.

[2] O. Strelow, Eine allgemeine Berechnungsmethode für Wärmeübertragerschaltungen, Forschung im Ingenieurwesen 63 (1997) 255–261.

[3] W. Roetzel, Transient analysis in heat exchangers (Presented at the 1993 ICHMT International Symposium on New Developments in Heat Exchangers, Lisbon, Portugal, September, 6–9, 1993), in: N. Afgan, et al. (Eds.), New Developments in Heat Exchangers, Gordon and Breach, Amsterdam, 1996, pp. 547–575, ISBN 90-5699-512-X.

[4] W. Roetzel, Y. Xuan, Dynamic Behaviour of Heat Exchangers, WIT Press, Boston, 1999.

[5] M. Meierer, N. Eimer, Langzeiterfahrung bei Betrieb, Instandhaltung und Optimierung des Wärmeverschiebesystems in einer Rauchgasentschwefelungsanlage, VGB Kraftwerkstechnik 9 (2000) 56–61.

[6] H. Schartmann, Wärmerückgewinnung in RLT-Anlagen mit Abluftbefeuchtung, Luft- und Kältetechnik 3 (1996) 115–119.

[7] A.L. London, W.M. Kays, The liquid-coupled indirect-transfer regenerator for gas-turbine Plants, Trans. ASME 73 (1951) 529–542.

[8] W.M. Kays, A.L. London, Hochleistungswärmeübertrager, Akademie Verlag, Berlin, 1973.

[9] K.-U. Schneider, Gasturbinen–Heizkraftwerke mit Flüssigmetall-Wärmeverschiebesystem, in: M. Tuma (Ed.), Proceedings of the International Symposium Gas Turbines and Gas Cycle Plants, May 27–28, 1993, University of Ljubljana, Faculty of Mechanical Engineering, Bled, Slovenia, 1993, ISBN 86–7217101-2.

[10] H. Martin, Wärmeübertrager, Georg Thieme Verlag, Stuttgart, 1988.

[11] W. Roetzel, Thermische Auslegung von Wärmeübertragersystemen mit umlaufendem Wärmeträger, BWK 42 (5) (1990) 254–258.

[12] W. Jansing, J. Klemm, H. Teubner, Flüssigmetall-Wärmeverschiebesystem für Gasturbinen–Heizkraftwerke, in: M. Tuma (Ed.), Proceedings of the International Symposium Gas Turbines and Gas Cycle Plants, May 27–28, 1993, University of Ljubljana, Faculty of Mechanical Engineering, Bled, Slovenia, 1993, ISBN 86–7217101-2.

[13] B. Spang, Wärmedurchgang und mittlere Temperaturdifferenz in Rekuperatoren, Habilitationsschrift, Universität der Bundeswehr Hamburg 1998, internet publication: http://www.unibw-hamburg.de/MWEB/ift/ftd/netzpub/spanghabil.pdf.

[14] D. Franke, Systeme mit Örtlich Verteilten Parametern, Springer-Verlag, Berlin, 1987.

[15] B. Davies, Integral Transforms and Their Applications, Springer-Verlag, New York, 1978.

[16] M.R. Spiegel, Laplace Transforms, McGraw-Hill, New York, 1965.

[17] G. Honig, Zur numerischen Lösung partieller Differentialgleichungen mit Laplace-transformation, Berichte der Kernforschungsanstalt Jülich, Jülich, 1978.

[18] J.W. Thomas, Numerical Partial Differential Equations: Finite Difference Methods, Springer-Verlag, New York, 1995.

[19] P. Duchateau, D.W. Zachmann, Partial Differential Equations, McGraw-Hill, Singapore, 1986.

[20] Ch. Na Ranong, Stationäres und instationäres Verhalten von zwei gekoppelten Wärmeübertragern mit umlaufendem Fluidstrom, Ph.D. Thesis, Universität der Bundeswehr Hamburg, Germany, 2001.

[21] O. Föllinger, Regelungstechnik, Hüthig Buch Verlag, Heidelberg, 1992.

[22] W. Oppelt, Kleines Handbuch technischer Regelvorgänge, 5th edn., Verlag Chemie, Weinheim, 1972.